© 2015. Published by The Company of Biologists Ltd | Development (2015) 142, 2633-2640 doi:10.1242/dev.121707

RESEARCH REPORT

Regulator of G-protein signaling 2 (RGS2) suppresses premature calcium release in mouse eggs

Miranda L. Bernhardt[1], Katie M. Lowther[2], Elizabeth Padilla-Banks[1], Caitlin E. McDonough[1], Katherine N. Lee[3], Alexei V. Evsikov[4], Tracy F. Uliasz[2], Peter Chidiac[3], Carmen J. Williams[1,*,‡] and Lisa M. Mehlmann[2,*,‡]

ABSTRACT

During oocyte maturation, capacity and sensitivity of Ca^{2+} signaling machinery increases dramatically, preparing the metaphase II (MII)-arrested egg for fertilization. Upon sperm-egg fusion, Ca^{2+} release from IP_3-sensitive endoplasmic reticulum stores results in cytoplasmic Ca^{2+} oscillations that drive egg activation and initiate early embryo development. Premature Ca^{2+} release can cause parthenogenetic activation prior to fertilization; thus, preventing inappropriate Ca^{2+} signaling is crucial for ensuring robust MII arrest. Here, we show that regulator of G-protein signaling 2 (RGS2) suppresses Ca^{2+} release in MII eggs. *Rgs2* mRNA was recruited for translation during oocyte maturation, resulting in ∼20-fold more RGS2 protein in MII eggs than in fully grown immature oocytes. *Rgs2*-siRNA-injected oocytes matured to MII; however, they had increased sensitivity to low pH and acetylcholine (ACh), which caused inappropriate Ca^{2+} release and premature egg activation. When matured *in vitro*, RGS2-depleted eggs underwent spontaneous Ca^{2+} increases that were sufficient to cause premature zona pellucida conversion. $Rgs2^{-/-}$ females had reduced litter sizes, and their eggs had increased sensitivity to low pH and ACh. $Rgs2^{-/-}$ eggs also underwent premature zona pellucida conversion *in vivo*. These findings indicate that RGS2 functions as a brake to suppress premature Ca^{2+} release in eggs that are poised on the brink of development.

KEY WORDS: RGS2, G_q, Oocyte, Meiotic maturation, Calcium, Egg activation

INTRODUCTION

Fully grown mammalian oocytes are arrested in meiotic prophase until a mid-cycle release of luteinizing hormone from the pituitary stimulates resumption of meiosis to the metaphase II (MII) stage, referred to herein as eggs. Fusion of the egg and sperm at fertilization introduces into the egg cytoplasm a sperm-specific phospholipase C (PLCζ) (Kashir et al., 2014), which initiates inositol 1,4,5-trisphosphate (IP_3)-mediated Ca^{2+} release from intracellular stores. An initial, prolonged rise in cytoplasmic Ca^{2+} is followed by several hours of repetitive, low-frequency Ca^{2+} oscillations (Runft et al., 2002). These Ca^{2+} oscillations drive the conversion of the egg to an early embryo by causing a series of downstream responses, including resumption of meiosis, cortical granule exocytosis, which prevents polyspermy, and recruitment of maternal mRNAs needed for successful embryonic development (Ducibella and Fissore, 2008).

During meiotic maturation, oocytes undergo several cytoplasmic changes that dramatically increase the ability of mature eggs to release Ca^{2+} in response to sperm or exogenous signals (Fujiwara et al., 1993; Jones et al., 1995; Mehlmann and Kline, 1994). These changes include an approximately fourfold increase in Ca^{2+} stores (Tombes et al., 1992), an increase in IP_3 receptor protein levels by 1.5- to twofold (Fissore et al., 1999; Mehlmann et al., 1996) and reorganization of the endoplasmic reticulum (ER) towards the plasma membrane (FitzHarris et al., 2007; Mehlmann et al., 1995), which places the Ca^{2+} stores proximal to exogenous signals. Priming of the egg for Ca^{2+} release, although needed for proper Ca^{2+} signaling after fertilization, is also associated with the risk of parthenogenetic activation should Ca^{2+} signals occur prior to sperm-egg fusion. Indeed, activation of overexpressed G_q-protein-coupled muscarinic receptors in mouse eggs by exogenous ligands in the absence of sperm causes IP_3-mediated Ca^{2+} release, Ca^{2+} oscillations and parthenogenetic egg activation (Moore et al., 1993; Williams et al., 1998, 1992). Ca^{2+} signaling prevents subsequent fertilization by inducing cortical granule release, which modifies the zona pellucida (ZP), a proteoglycan-rich extracellular matrix that surrounds the egg, to cause the 'block to polyspermy'.

Because the mature egg is exceedingly sensitive to stimuli that can activate IP_3-mediated Ca^{2+} release via G-protein-coupled receptors, we reasoned that a mechanism was in place to suppress this response prior to sperm-egg fusion. Regulator of G-protein signaling (RGS) proteins are a ubiquitous family of proteins that downregulate G-protein-coupled receptor signaling by inhibiting the activity of G-proteins (Heximer and Blumer, 2007). In general, RGS proteins stimulate the hydrolysis of GTP bound to activated Gα subunits, leading to signal termination (Willars, 2006). Here, we tested the hypothesis that RGS2, which inhibits both G_q and G_s signaling (Ingi et al., 1998; Roy et al., 2006; Wang et al., 2004), suppresses Ca^{2+} release in mature mouse eggs. We report that RGS2 translation during meiotic maturation serves as a safety mechanism to prevent parthenogenetic egg activation prior to fertilization.

RESULTS AND DISCUSSION

RGS2 protein levels increase during oocyte maturation

To determine which RGS proteins are expressed in mouse oocytes, we searched an oocyte gene expression database (Evsikov et al., 2006). Among RGS isoforms, RGS2 had the highest expression levels, ∼500 transcripts per million (Blake et al., 2014). *Rgs2* mRNA was highly expressed in germinal vesicle (GV)-stage oocytes, decreased during oocyte maturation and was greatly reduced at the 2-cell stage (Fig. 1A). By contrast, RGS2 protein was

[1]Reproductive and Developmental Biology Laboratory, National Institute of Environmental Health Sciences, National Institutes of Health, Research Triangle Park, NC 27709, USA. [2]Department of Cell Biology, UConn Health, Farmington, CT 06030, USA. [3]Department of Physiology and Pharmacology, Schulich School of Medicine and Dentistry, University of Western Ontario, London, Ontario, Canada N6A 5C1. [4]Department of Molecular Medicine, University of South Florida, Tampa, FL 33612, USA.
*These authors contributed equally to this work

‡Authors for correspondence (williamsc5@niehs.nih.gov; lmehlman@uchc.edu)

Received 5 January 2015; Accepted 25 June 2015

Development (2015) 142, 2633-2640 doi:10.1242/dev.121707

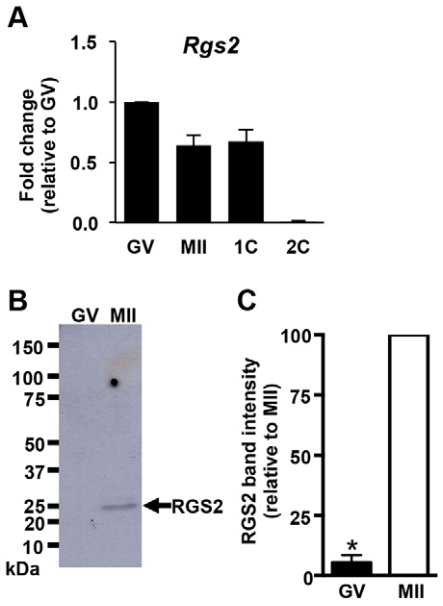

Fig. 1. RGS2 expression in oocytes, eggs and early embryos. (A) *Rgs2* mRNA levels; all stages expressed relative to GV oocytes. *N*=3; graph shows mean±s.e.m. (B) Immunoblot of RGS2 protein in oocytes and eggs. Blot representative of 4 independent replicates; 50 oocytes or eggs/lane. (C) Quantitation of RGS2 immunoblot signal. *N*=4; graph shows mean±s.e.m. **P*<0.05, Mann–Whitney test. GV, GV-stage oocytes; MII, MII eggs; 1C, 1-cell embryos; 2C, 2-cell embryos.

minimally detected in GV oocytes but increased ~20-fold during maturation to the MII stage (Fig. 1B,C). These findings indicate that RGS2 is developmentally regulated and suggest that it functions during oocyte maturation or beyond.

Exposure to acidic pH causes spontaneous activation in eggs lacking RGS2

To test functional roles of RGS2, we used both overexpression and knockdown approaches. Because G_s activity is crucial for the maintenance of prophase arrest prior to oocyte maturation (Mehlmann et al., 2002, 2004), and RGS2 can inhibit the activity of G_s (Roy et al., 2006, 2003; Sinnarajah et al., 2001), we first tested whether altering RGS2 levels affected maturation success. Overexpressing RGS2 in GV oocytes did not stimulate meiotic resumption, and depleting RGS2 in oocytes using RNA interference did not affect the progression of meiosis or meiotic spindle formation (Fig. 2A,B; see supplementary material Table S1 and Fig. S1). These results suggest that RGS2 is not required during oocyte maturation and that these approaches could be used to examine its function in MII eggs.

RGS2 potently suppresses G_q signaling (Ingi et al., 1998; Wang et al., 2004), and, in mouse eggs, activation of G_q in the absence of sperm leads to Ca^{2+}-mediated resumption of meiosis and complete egg activation (Moore et al., 1993; Williams et al., 1998). Sperm do not appear to utilize this pathway (Williams et al., 1998) but instead stimulate IP_3 generation directly by introducing PLCζ (Saunders et al., 2002; Knott et al. 2005). However, G_q activation triggers the same downstream IP_3 receptor-mediated Ca^{2+} release that is essential for fertilization. To determine whether RGS2 activity could impact Ca^{2+} signals at fertilization, we tested the effect of RGS2 depletion on Ca^{2+} oscillatory patterns during *in vitro* fertilization (IVF). We found that RGS2-depleted eggs exhibited normal Ca^{2+} oscillations, with the exception that the duration of the first Ca^{2+} transient was slightly, but consistently, shorter (see supplementary material Fig. S2A-D). This finding suggests that the Ca^{2+} stores were depleted prior to fertilization, which could be explained by either impaired Ca^{2+} store accumulation during maturation or by premature Ca^{2+} release. To distinguish between these possibilities, we analyzed Ca^{2+} stores in control and RGS2-depleted MII eggs by measuring thapsigargin-mediated ER Ca^{2+} release. There was no difference in Ca^{2+} stores between control and RGS2-depleted MII eggs when the ZPs were intact (see supplementary material Fig. S2E-G).

As is typical for IVF experiments, the ZP was removed prior to insemination to promote rapid synchronous fertilization during Ca^{2+} imaging. We noticed that many ZP-free, RGS2-depleted eggs began emitting second polar bodies before sperm addition (Fig. 2C), indicating spontaneous activation. Spontaneous activation was only observed in ZP-free RGS2-depleted eggs, not in ZP-intact eggs (see supplementary material Fig. S3A). Our standard protocol for ZP removal is a brief treatment with acid Tyrode's medium. We therefore tested whether absence of the ZP or the acid exposure was causing the spontaneous activation by using pronase treatment as an alternative method for ZP removal. Pronase-treated eggs did not activate, whereas eggs exposed to acid had high rates of second polar body emission, and most of the activated eggs went on to form pronuclei or to cleave (Fig. 2D; see supplementary material Fig. S3A-D). These findings are consistent with previous observations of acid induction of parthenogenetic activation in mouse and human eggs (Johnson et al., 1990). In addition, spontaneous Ca^{2+} changes were observed in 25% (4/16) of the siRNA-injected cells prior to addition of sperm, but never (0/15) in controls (see supplementary material Fig. S3E). These Ca^{2+} changes could explain the shortened first transients of eggs lacking RGS2, because premature Ca^{2+} release would result in Ca^{2+} store depletion prior to fertilization. To test this idea, we analyzed Ca^{2+} stores in ZP-free control and RGS2-depleted MII eggs. Ca^{2+} stores were significantly lower in RGS2-depleted eggs when the ZPs were removed using acid Tyrode's medium, but not different when the ZPs were removed by manual microdissection (see supplementary material Fig. S3F-H). Taken together, these findings indicate that lack of RGS2 during oocyte maturation does not affect Ca^{2+} accumulation into ER stores, and suggest that acid-induced premature Ca^{2+} release in RGS2-depleted eggs causes a reduction in Ca^{2+} stores and, as a consequence, shortened first Ca^{2+} transients following fertilization.

Acidic pH induces a rise in intracellular Ca^{2+} in eggs lacking RGS2 but not in control eggs

To characterize the acid sensitivity of RGS2-depleted eggs, we examined the effect of gradually lowering pH on Ca^{2+} release. The majority of control eggs treated with acid did not exhibit increases in Ca^{2+} even at a pH as low as 5 (Fig. 2E,F). However, most RGS2-depleted eggs showed marked increases in Ca^{2+} starting between pH 6.2 and 6.9, suggesting that RGS2 inhibits acid-induced Ca^{2+} release. Similar results were obtained using an *Rgs2*-targeted morpholino oligonucleotide (Fig. 2G), indicating that this response was not due to a non-specific effect of siRNA.

We also examined the Ca^{2+} response to increased acid in GV-stage oocytes, which have low levels of RGS2 protein, and throughout oocyte maturation. We found that GV- and GVBD-stage oocytes (maturing oocytes that have undergone nuclear envelope breakdown) were very sensitive to lower pH, with virtually all oocytes displaying Ca^{2+} release starting at pH 6.4-6.6 (Fig. 3A,B). Acid sensitivity decreased during maturation such that fewer

Development (2015) 142, 2633-2640 doi:10.1242/dev.121707

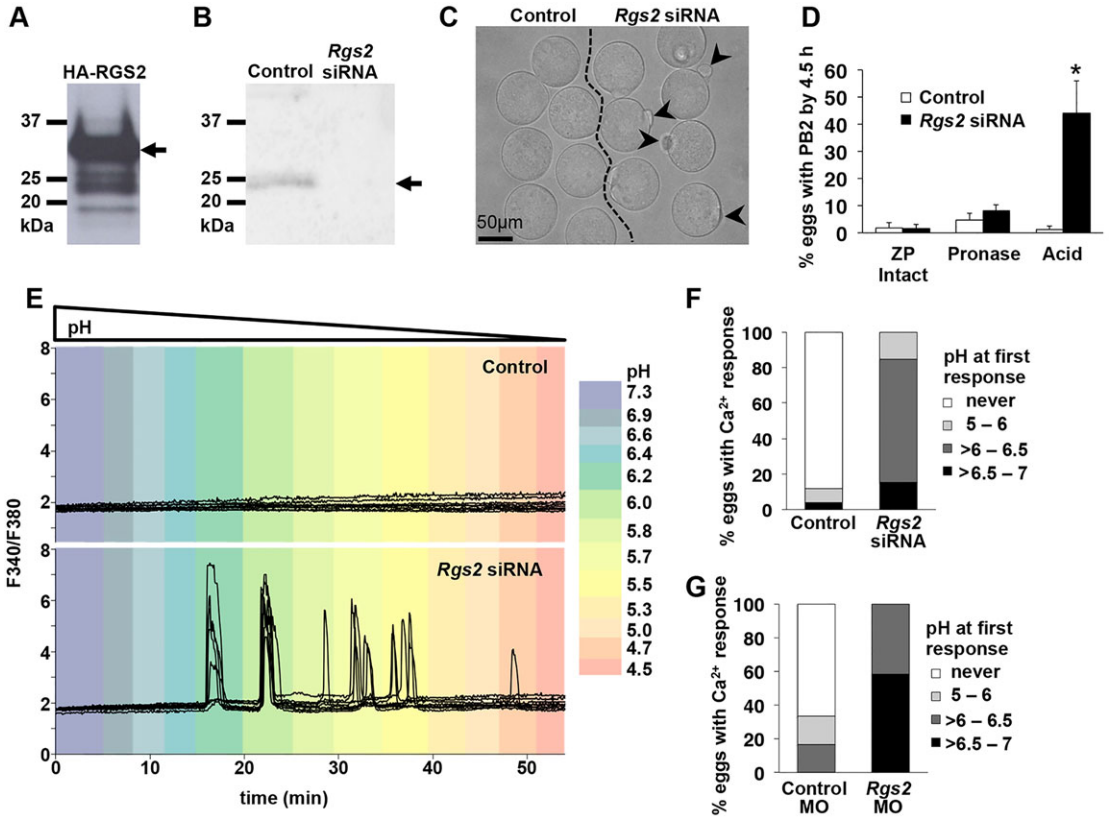

Fig. 2. Acid-induced Ca^{2+} release causes resumption of meiosis in eggs lacking RGS2 protein. (A) Immunoblot of GV oocytes following microinjection with cRNA encoding HA-tagged RGS2, probed with monoclonal anti-RGS2 antibody. Arrow, full-length HA-RGS2 band. 20 oocytes/lane. (B) Immunoblot of RGS2 in control MII eggs or eggs matured to MII following microinjection at the GV stage with *Rgs2* siRNA. 20 eggs/lane. Arrow, RGS2 band. (C) Appearance of siRNA-injected eggs following ZP removal with acid Tyrode's solution. Eggs in different groups are separated by dashed line. Arrowheads indicate second polar bodies. (D) Average percentage of eggs with second polar body (PB2) emitted by 4.5 h after the indicated treatment. *N*=5 independent replicates with 8-27 cells per group/replicate; graph shows mean±s.e.m. **P*<0.05, ANOVA with Bonferroni's multiple comparison test. (E) Relative level of intracellular Ca^{2+} in response to lowering pH in control eggs or eggs lacking RGS2. Color indicates approximate pH at each time point. Eight representative tracings shown/group. (F) Percentage of siRNA-injected eggs with a rise in intracellular Ca^{2+} beginning at the indicated pH. (G) Percentage of morpholino (MO)-injected eggs with a rise in intracellular Ca^{2+} beginning at the indicated pH. Control MO, scrambled MO; *Rgs2* MO, *Rgs2*-targeted MO. Graphs in F and G indicate cumulative percentage of 3-8 cells/group from *n*=4 or *n*=2 experiments, respectively.

metaphase I oocytes and MII-stage eggs responded to lower pH with Ca^{2+} release (Fig. 3A,B). This decrease in sensitivity during maturation correlated with increased translation of *Rgs2*. To examine directly the role of RGS2 in inhibiting acid-induced Ca^{2+} release, we overexpressed RGS2 protein in GV-stage oocytes and tested their response to acid treatment. Control oocytes released Ca^{2+} in response to lowering pH beginning at pH 6.4-6.6. By contrast, RGS2-overexpressing oocytes had a greatly reduced Ca^{2+} response, with fewer cells responding, and the total amount of Ca^{2+} released being much lower when Ca^{2+} release occurred at all (Fig. 3C,D).

In somatic cells, RGS2 inhibits acid-induced responses, such as those induced by alterations in pH that result from inflammatory conditions including asthma (Liu et al., 2013). Studies in airway epithelial cells suggest that lower pH activates the G_q-coupled proton sensor GPR68 (also called OGR1) to release Ca^{2+}, which stimulates the production of MUC5AC (Liu et al., 2013; Ludwig et al., 2003; Saxena et al., 2012). RGS2 overexpression prevents acid-induced secretion of MUC5AC, and RGS2 depletion increases this response (Liu et al., 2013). These results indicate that RGS2 acts as an inhibitory regulator of acid-induced cellular responses by binding to G_q. GPR68 or a similar receptor could act as a proton sensor linked to Ca^{2+} signaling by activating G_q in oocytes. Indeed, GV-stage oocytes have significant levels of *Gpr68* transcripts compared with those in MII eggs and early embryos (Fig. 3E). It is unclear whether mouse eggs are exposed to low pH under physiological conditions within the ovarian follicle or oviduct, as direct measurements have not been reported. In larger species, follicular fluid and oviduct pH is generally in the range of 7-8 [reviewed by Edwards (1974); Stone and Hamner (1975)], but pH has been measured as low as 6.8 in bovine follicles and pig oviducts (Smiljaković et al., 2008; Zachariae and Jensen, 1958). In addition, follicle or oviductal pH could drop during an inflammatory process as has been observed in inflamed airways (Liu et al., 2013).

Acetylcholine causes Ca^{2+} release in oocytes and RGS2-depleted eggs

In addition to an acidic environment, eggs could be exposed to other stimuli that activate G_q *in vivo*. One such stimulus is acetylcholine (ACh). Choline acetyltransferase, which synthesizes ACh, is expressed in granulosa cells from large antral follicles of human, monkey and rat ovaries (Fritz et al., 1999, 2001; Mayerhofer et al., 2006). Moreover, ACh has been measured in cultured human and rat granulosa cells (Fritz et al., 2001) and in adult rat ovaries (Mayerhofer et al., 2006). Interestingly, the amount of ACh in rat granulosa cells is significantly increased by follicle stimulating

Development (2015) 142, 2633-2640 doi:10.1242/dev.121707

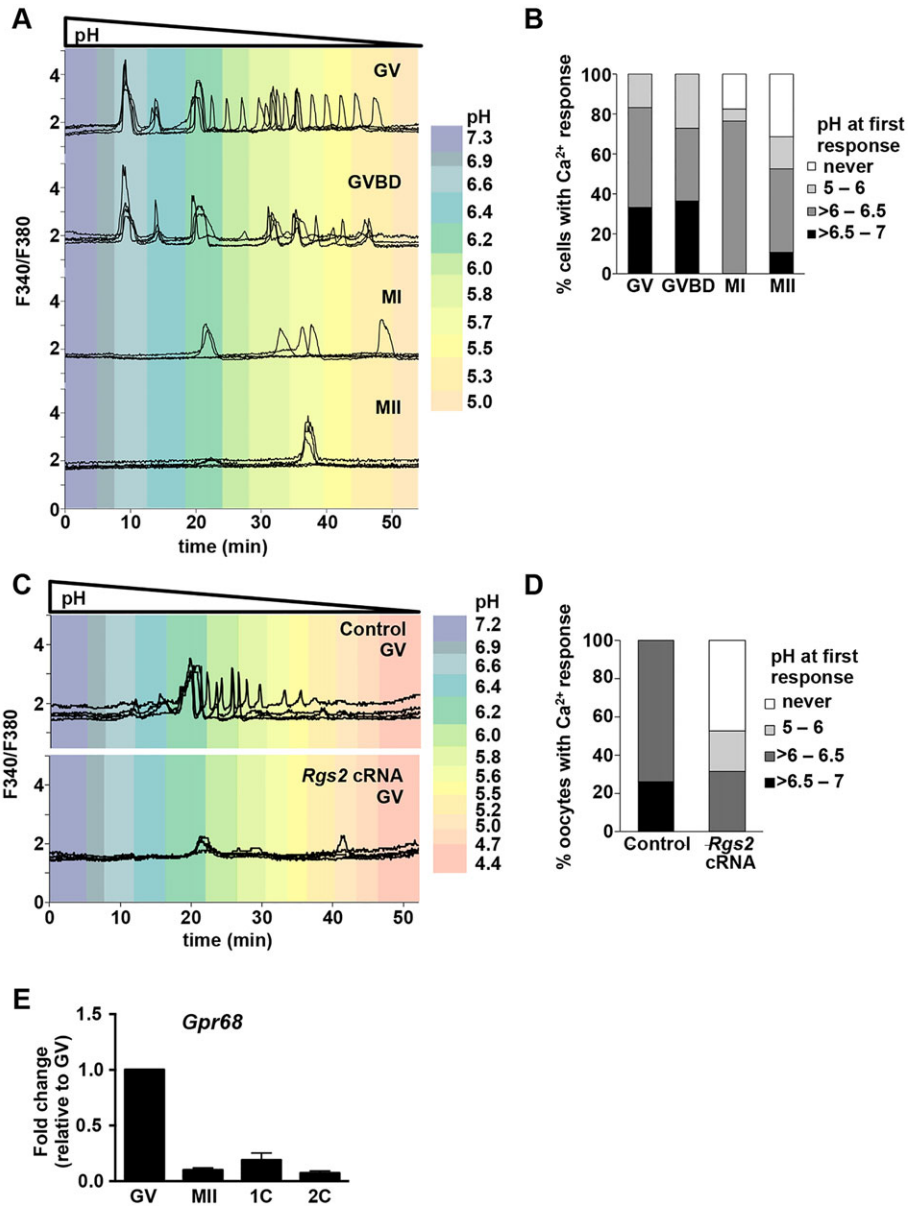

Fig. 3. RGS2 mediates loss of acid-induced Ca^{2+} response during oocyte maturation. (A) Relative level of intracellular Ca^{2+} in response to lowering pH in maturing oocytes. Graphs show 4-5 representative tracings/group. (B) Percentage of oocytes with a rise in intracellular Ca^{2+} beginning at the indicated pH. Graph indicates cumulative percentage of 2-5 cells/group from *n*=5 independent replicates. (C) Relative level of intracellular Ca^{2+} in response to lowering pH in control GV oocytes or GV oocytes overexpressing RGS2 (*Rgs2* cRNA). Six representative tracings/group. (D) Percentage of oocytes with a rise in intracellular Ca^{2+} beginning at the indicated pH levels. Graph indicates cumulative percentage of 3-8 cells/group from *n*=4 independent replicates. (E) *Gpr68* mRNA level; all stages expressed relative to GV oocytes. *N*=3; graph shows mean± s.e.m. GV, GV oocyte; GVBD, oocytes immediately following GV breakdown; MI, metaphase I stage; MII, MII eggs; 1C, 1-cell embryos; 2C, 2-cell embryos.

hormone (Mayerhofer et al., 2006), suggesting that maturing oocytes are exposed to ACh *in vivo*. ACh treatment stimulates Ca^{2+} release via G_q-coupled muscarinic receptors, which are expressed in oocytes of several species including mouse (Caratsch et al., 1984; Eusebi et al., 1979, 1984). In addition, stimulation of the muscarinic receptor induces Ca^{2+} release in immature growing mouse oocytes (Carroll et al., 1994) but not in MII eggs (Williams et al., 1998).

We examined the ability of ACh to stimulate Ca^{2+} release in oocytes, eggs and RGS2-depleted eggs. All of the GV-stage oocytes and RGS2-depleted eggs released Ca^{2+} in response to addition of ACh, whereas the majority of control eggs that contained RGS2 showed no response (Fig. 4A,B). Treatment of GV-stage oocytes with the muscarinic receptor antagonist atropine almost completely suppressed ACh-induced Ca^{2+} release (Fig. 4C), but did not affect acid-induced Ca^{2+} release (data not shown). These findings indicate that RGS2 effectively inhibits G_q-mediated Ca^{2+} release in response to ACh, and suggest that one function of the maturation-associated accumulation of RGS2 protein is to suppress this physiological response.

RGS2-depleted eggs undergo premature ZP conversion

Ca^{2+} release at fertilization triggers cortical granule exocytosis and release of the protease ovastacin, which cleaves the ZP protein ZP2 to $ZP2_f$ (Burkart et al., 2012). This cleavage event is responsible for the ZP block to polyspermy. Because cortical granule release in eggs is easily triggered in response to rises in cytoplasmic Ca^{2+} (Ducibella et al., 2002), ZP2 cleavage can be used as a proxy for Ca^{2+} release over time. To test whether RGS2 regulates Ca^{2+} release during oocyte maturation, we microinjected GV-stage oocytes with *Rgs2* siRNA, matured them and then measured the percentage of ZP2-to-$ZP2_f$ conversion. RGS2-depleted eggs consistently had elevated levels of ZP2 conversion compared with controls (Fig. 4D,E). These findings demonstrate that during *in vitro* maturation of RGS2-depleted oocytes, Ca^{2+} increases occurred that were sufficient to cause cortical granule release and promote ZP2 conversion.

A full RGS2 knockout mouse has been developed and this mouse has at least two defects due to inappropriate Ca^{2+} regulation. RGS2 knockout pancreatic acinar cells have significantly higher IP_3-mediated Ca^{2+} release in response to muscarinic receptor activation

Development (2015) 142, 2633-2640 doi:10.1242/dev.121707

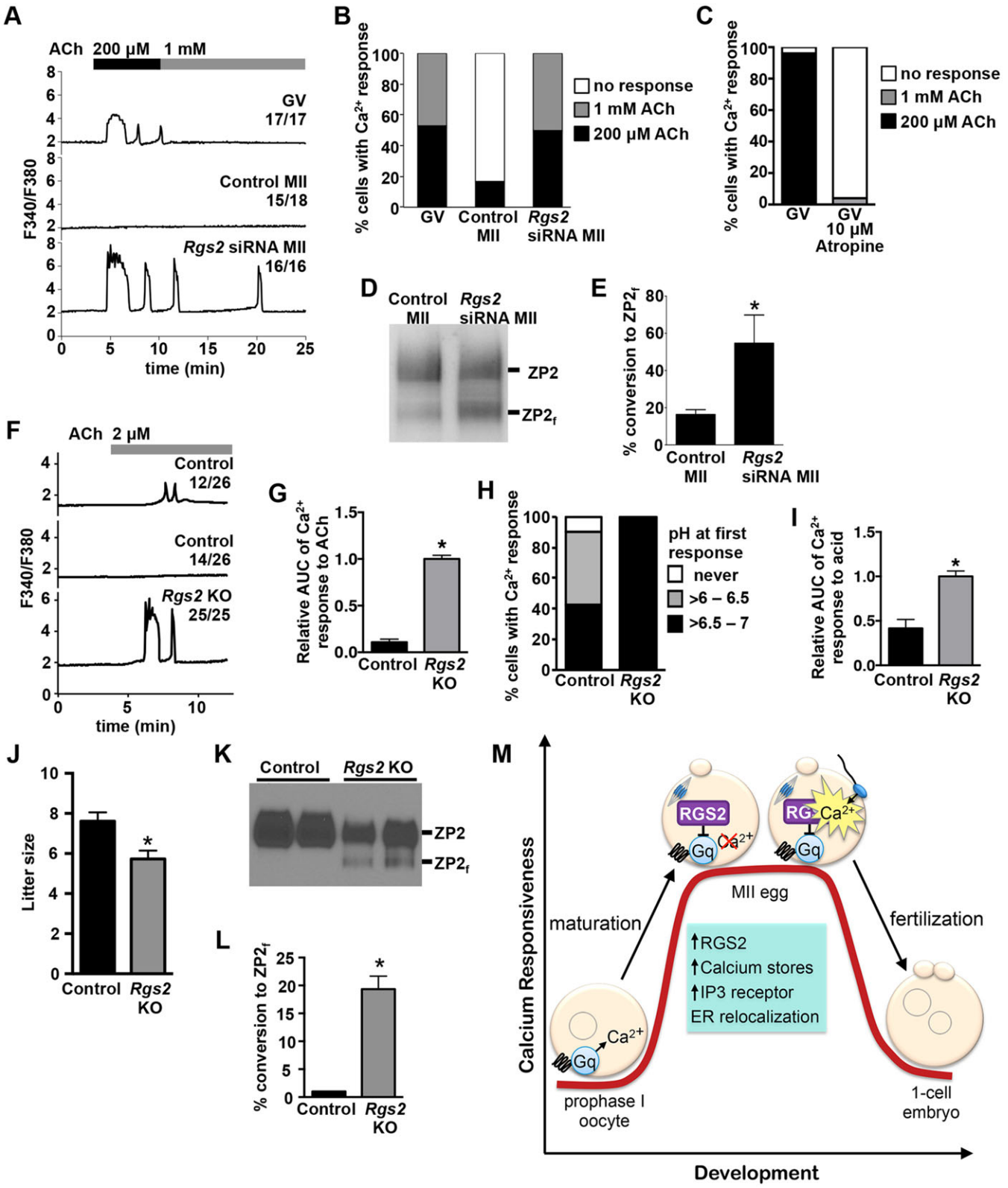

Fig. 4. See next page for legend.

(Wang et al., 2004). In addition, these knockout mice have high blood pressure due to increased Ca^{2+} release in response to vasoconstrictors, which act through G_q-coupled receptors. To determine whether loss of RGS2 *in vivo* resulted in abnormal responses to G-protein-coupled receptor agonists, we tested the effects of ACh and acidic pH on MII eggs from *Rgs2*$^{+/+}$ and *Rgs2*$^{-/-}$ females. Consistent with our findings in RGS2-depleted eggs, 100% of the *Rgs2*$^{-/-}$ eggs responded to ACh by releasing Ca^{2+}

Development (2015) 142, 2633-2640 doi:10.1242/dev.121707

Fig. 4. RGS2 inhibits acetylcholine (ACh)-induced Ca^{2+} release and premature ZP2 cleavage. (A) Relative level of intracellular Ca^{2+} in response to the indicated ACh concentrations. One representative tracing is shown per group, along with the proportion of cells displaying a similar pattern. GV, GV oocytes; Control MII, *in vitro*-matured MII eggs; *Rgs2* siRNA MII, MII eggs matured *in vitro* following microinjection at the GV stage with *Rgs2* siRNA. (B) Percentage of cells with a rise in intracellular Ca^{2+} beginning at the indicated ACh concentrations. Graph indicates cumulative percentage of 4-6 cells/group from n=4 independent replicates. (C) Effect of atropine on ACh-induced Ca^{2+} response in GV oocytes. Graph indicates cumulative percentage of 25 cells/group from n=3 independent replicates. (D) Immunoblot of ZP2 protein. Oocytes were microinjected with scrambled siRNA (control) or *Rgs2* siRNA, then matured *in vitro* to MII. Blot represents 3 independent replicates; 12 eggs per lane. ZP2, full-length ZP2 protein; $ZP2_f$, cleaved form of ZP2. (E) Quantitation of ZP2-to-$ZP2_f$ conversion. Graph shows mean±s.e.m. of 3 independent replicates. *P<0.05; t-test. (F) Relative level of intracellular Ca^{2+} in response to 2 µM ACh. Representative tracings are shown along with the proportion of cells displaying a similar pattern. Control, $Rgs2^{+/+}$ eggs; *Rgs2* KO, $Rgs2^{-/-}$ eggs. (G) Relative area under the curve (AUC) of ACh response. N=25-26 total eggs in 5 independent experiments. Graph shows mean±s.e.m. *P<0.05, t-test. (H) Number of eggs with a rise in intracellular Ca^{2+} beginning at the indicated pH. (I) Relative AUC of acid response. N=21-23 total eggs in 4 independent experiments. Graph shows mean±s.e.m. *P<0.05, t-test. (J) Average litter size for the indicated genotype. N=31-33 litters; *P<0.05, t-test. (K) Immunoblot of ZP2 protein from $Rgs2^{+/+}$ (control) and $Rgs2^{-/-}$ (*Rgs2* KO) eggs. Blot shows 2 of 3 replicates; 10 eggs per lane. (L) Quantitation of ZP2-to-$ZP2_f$ conversion in the indicated groups. Graph shows mean±s.e.m. of 3 replicates. *P<0.05; t-test. (M) Schematic summarizing RGS2 function after oocyte maturation in suppressing Ca^{2+} signaling mediated by G_q prior to fertilization.

(Fig. 4F). Only 12/26 $Rgs2^{+/+}$ eggs showed some degree of response to ACh, but far less Ca^{2+} was released than in $Rgs2^{-/-}$ eggs (Fig. 4G). Similarly, $Rgs2^{-/-}$ eggs responded at a higher pH and released more Ca^{2+} than $Rgs2^{+/+}$ eggs (Fig. 4H,I). Of note, control eggs in these experiments, which were from C57BL/6J females, were more sensitive to both ACh and acid when compared with the CF-1 eggs used in previous experiments, as demonstrated by the greater proportion showing responses. These findings draw attention to mouse strain differences that probably underlie conflicting reports regarding responses of MII eggs to ACh (Kang et al., 2003; McGuinness et al., 1996; Williams et al., 1992). In fact, the MF-1 mouse strain, which produces eggs that have a high incidence of activation following acid-mediated ZP removal (Johnson et al., 1990), was the subject of a quantitative trait locus analysis that identified the *Rgs2* gene locus as a modulator of anxiety (Yalcin et al., 2004). These findings suggest that differences in RGS2 expression or function contribute to the increased sensitivity of MF-1 eggs to ACh and acid activation.

RGS2 knockout mice are viable and fertile, but no formal breeding study has been reported. We analyzed litter sizes from ongoing production of $Rgs2^{+/+}$ and $Rgs2^{-/-}$ mice over a 32-month period. The average litter size of $Rgs2^{-/-}$ females was significantly lower than that of $Rgs2^{+/+}$ females (Fig. 4J). This finding was due to subfertility of the $Rgs2^{-/-}$ females, because litters of $Rgs2^{+/+}$ females mated to $Rgs2^{-/-}$ males were not smaller than those of wild-type pairs (data not shown). A possible explanation for the reduced litter size was premature cleavage of ZP2 similar to that observed in RGS2-depleted eggs, which could result in impaired fertilization. To test this idea, we collected MII eggs from $Rgs2^{+/+}$ and $Rgs2^{-/-}$ females 16 h after hCG administration and quantified ZP2-to-$ZP2_f$ conversion. Indeed, $Rgs2^{-/-}$ eggs had increased levels of ZP2 conversion compared with those from $Rgs2^{+/+}$ females (Fig. 4K,L). These findings indicate that RGS2 suppresses Ca^{2+} release *in vivo*. The finding that the mice were not completely infertile suggests that, in addition to RGS2, other mechanisms are in place to help prevent premature Ca^{2+} release.

In conclusion, a dramatic rise in intracellular Ca^{2+} is of paramount importance for successful egg activation and embryo development in all animals (Kashir et al., 2013). Mammalian oocytes do not develop the ability to efficiently release large amounts of Ca^{2+} until immediately before ovulation, thereby preventing premature Ca^{2+} release that could preclude successful fertilization. As the oocyte becomes fertilization-competent, it is exquisitely sensitive to signals that release Ca^{2+} (Fig. 4M). Our findings suggest that RGS2 functions to inhibit premature G-protein-mediated Ca^{2+} release in eggs that are poised for activation by PLCζ from the fertilizing sperm.

MATERIALS AND METHODS

Gamete collection and oocyte microinjection

All mice used (see details in the supplementary Materials and Methods) were maintained under approved protocols and complied with the Institute of Laboratory Animal Research Guide for the Care and Use of Laboratory Animals. Oocytes, eggs, embryos and sperm were collected and oocytes were microinjected with 5-10 pl volume, essentially as previously described (Bernhardt et al., 2011; Jefferson et al., 2009). Pipette concentrations of microinjected reagents were as follows: *Rgs2* siRNA (Ambion) and control nontargeting siRNA (Santa Cruz), 2 µM; *Rgs2* and control morpholinos (GeneTools), 2 mM; and HA-RGS2 cRNA, 1 µg/µl. siRNA- and morpholino-injected oocytes were cultured in 10 µM milrinone for 5-8 h to allow protein turnover and then matured. cRNA-injected oocytes were incubated in milrinone-containing medium for 18-20 h prior to imaging to allow for protein overexpression. For some experiments, ZPs were removed by brief exposure to acidic Tyrode's solution, pH 1.6, by incubation for 4-8 min in 5 mg/ml pronase, or by piezoelectric-actuated drilling of a 50-µm slit in the ZP, followed by gentle pipetting using a 70-µm inner diameter capillary. Culture media used are detailed in the supplementary Materials and Methods.

Calcium imaging

Ca^{2+} imaging was performed as previously described (Miao et al., 2012). For fertilization experiments, ZP-free eggs were adhered to Cell-Tak-coated dishes in BSA-free medium under mineral oil. Capacitated sperm were added to a final concentration of 10^5 sperm/ml. For acid addition and ACh experiments, ZP-intact cells were used. HCl (1 N) was diluted 1:100, and 150 µl of this solution was added to 2 ml medium several minutes apart during imaging. pH measurements were made using parallel additions of the dilute HCl to the same medium volume. ACh was prepared as a 5 mM stock in water and added to L-15 medium during imaging to achieve final concentrations of 2 µM, 200 µM and 1 mM.

Immunofluorescence and immunoblotting

For spindle staining, eggs were fixed, extracted and blocked as previously described (Bernhardt et al., 2012). Oocytes, eggs or embryos were lysed in sample buffer, separated under reducing conditions and immunoblotted as previously described (Jefferson et al., 2013). Details regarding antibodies are provided in the supplementary Materials and Methods.

Real-time RT-PCR

Total RNA was isolated from 50 oocytes, eggs or embryos using an Arcturus Pico Pure kit (Life Technologies). EGFP cRNA was generated as previously described (Miao et al., 2012) and 10 pg was added to each sample prior to RNA isolation as an internal control. Real-time RT-PCR was performed as previously described (Jefferson et al., 2013), using cDNA from two oocytes or embryos per reaction. Primer sequences are provided in the supplementary Materials and Methods. Relative gene expression was calculated by the ΔCt method (Pfaffl, 2001) using EGFP expression for normalization.

Statistical analysis

Data were analyzed using one-way ANOVA, Student's *t*-test, Mann–Whitney *U*-test or chi-square test, as indicated in the figure legends. Statistical tests were performed using GraphPad Prism.

Acknowledgements

We thank Yaping Tu for providing *Rgs2*$^{-/-}$ mice, Dean Betts and Nicole Edwards for obtaining *Rgs2*$^{-/-}$ eggs, Jurrien Dean for the ZP2 antibody, and Laurinda Jaffe and Bruce White for helpful discussions.

Competing interests

The authors declare no competing or financial interests.

Author contributions

M.L.B., K.M.L., P.C., C.J.W. and L.M.M. designed the experiments. M.L.B., K.M.L., E.P.-B., C.E.M., K.N.L., A.V.E., T.F.U. and L.M.M. performed the experiments and analyzed the data. M.L.B., C.J.W. and L.M.M. wrote the manuscript. All authors edited and approved the final manuscript.

Funding

This work was supported by the Intramural Research Program of the National Institutes of Health (NIH), National Institute of Environmental Health Sciences [Z01ES102985 to C.J.W.], NIH grant HD056366 and the University of Connecticut Health Center Research Advisory Council (to L.M.M.), and a grant from the Canadian Institutes of Health Research (to P.C.). Deposited in PMC for release after 12 months.

Supplementary material

Supplementary material available online at
http://dev.biologists.org/lookup/suppl/doi:10.1242/dev.121707/-/DC1

References

Bernhardt, M. L., Kim, A. M., O'Halloran, T. V. and Woodruff, T. K. (2011). Zinc requirement during meiosis I-meiosis II transition in mouse oocytes is independent of the MOS-MAPK pathway. *Biol. Reprod.* **84**, 526-536.

Bernhardt, M. L., Kong, B. Y., Kim, A. M., O'Halloran, T. V. and Woodruff, T. K. (2012). A zinc-dependent mechanism regulates meiotic progression in mammalian oocytes. *Biol. Reprod.* **86**, 114.

Blake, J. A., Bult, C. J., Eppig, J. T., Kadin, J. A. and Richardson, J. E. (2014). The Mouse Genome Database: integration of and access to knowledge about the laboratory mouse. *Nucleic Acids Res.* **42**, D810-D817.

Burkart, A. D., Xiong, B., Baibakov, B., Jimenez-Movilla, M. and Dean, J. (2012). Ovastacin, a cortical granule protease, cleaves ZP2 in the zona pellucida to prevent polyspermy. *J. Cell Biol.* **197**, 37-44.

Caratsch, C., Eusebi, F. and Salustri, A. (1984). Acetylcholine receptors in monkey and rabbit oocytes. *J. Cell. Physiol.* **121**, 415-418.

Carroll, J., Swann, K., Whittingham, D. and Whitaker, M. (1994). Spatiotemporal dynamics of intracellular [Ca2+]i oscillations during the growth and meiotic maturation of mouse oocytes. *Development* **120**, 3507-3517.

Ducibella, T. and Fissore, R. (2008). The roles of Ca2+, downstream protein kinases, and oscillatory signaling in regulating fertilization and the activation of development. *Dev. Biol.* **315**, 257-279.

Ducibella, T., Huneau, D., Angelichio, E., Xu, Z., Schultz, R. M., Kopf, G. S., Fissore, R., Madoux, S. and Ozil, J.-P. (2002). Egg-to-embryo transition is driven by differential responses to Ca(2+) oscillation number. *Dev. Biol.* **250**, 280-291.

Edwards, R. G. (1974). Follicular fluid. *J. Reprod. Fertil.* **37**, 189-219.

Eusebi, F., Mangia, F. and Alfei, L. (1979). Acetylcholine-elicited responses in primary and secondary mammalian oocytes disappear after fertilisation. *Nature* **277**, 651-653.

Eusebi, F., Pasetto, N. and Siracusa, G. (1984). Acetylcholine receptors in human oocytes. *J. Physiol.* **346**, 321-330.

Evsikov, A. V., Graber, J. H., Brockman, J. M., Hampl, A., Holbrook, A. E., Singh, P., Eppig, J. J., Solter, D. and Knowles, B. B. (2006). Cracking the egg: molecular dynamics and evolutionary aspects of the transition from the fully grown oocyte to embryo. *Genes Dev.* **20**, 2713-2727.

Fissore, R. A., Longo, F. J., Anderson, E., Parys, J. B. and Ducibella, T. (1999). Differential distribution of inositol trisphosphate receptor isoforms in mouse oocytes. *Biol. Reprod.* **60**, 49-57.

FitzHarris, G., Marangos, P. and Carroll, J. (2007). Changes in endoplasmic reticulum structure during mouse oocyte maturation are controlled by the cytoskeleton and cytoplasmic dynein. *Dev. Biol.* **305**, 133-144.

Fritz, S., Fohr, K. J., Boddien, S., Berg, U., Brucker, C. and Mayerhofer, A. (1999). Functional and molecular characterization of a muscarinic receptor type and evidence for expression of choline-acetyltransferase and vesicular acetylcholine transporter in human granulosa-luteal cells. *J. Clin. Endocrinol. Metab.* **84**, 1744-1750.

Fritz, S., Wessler, I., Breitling, R., Rossmanith, W., Ojeda, S. R., Dissen, G. A., Amsterdam, A. and Mayerhofer, A. (2001). Expression of muscarinic receptor types in the primate ovary and evidence for nonneuronal acetylcholine synthesis. *J. Clin. Endocrinol. Metab.* **86**, 349-354.

Fujiwara, T., Nakada, K., Shirakawa, H. and Miyazaki, S. (1993). Development of inositol trisphosphate-induced calcium release mechanism during maturation of hamster oocytes. *Dev. Biol.* **156**, 69-79.

Heximer, S. P. and Blumer, K. J. (2007). RGS proteins: Swiss army knives in seven-transmembrane domain receptor signaling networks. *Sci STKE* **2007**, pe2.

Ingi, T., Krumins, A. M., Chidiac, P., Brothers, G. M., Chung, S., Snow, B. E., Barnes, C. A., Lanahan, A. A., Siderovski, D. P., Ross, E. M. et al. (1998). Dynamic regulation of RGS2 suggests a novel mechanism in G-protein signaling and neuronal plasticity. *J. Neurosci.* **18**, 7178-7188.

Jefferson, W. N., Padilla-Banks, E., Goulding, E. H., Lao, S.-P. C., Newbold, R. R. and Williams, C. J. (2009). Neonatal exposure to genistein disrupts ability of female mouse reproductive tract to support preimplantation embryo development and implantation. *Biol. Reprod.* **80**, 425-431.

Jefferson, W. N., Chevalier, D. M., Phelps, J. Y., Cantor, A. M., Padilla-Banks, E., Newbold, R. R., Archer, T. K., Kinyamu, H. K. and Williams, C. J. (2013). Persistently altered epigenetic marks in the mouse uterus after neonatal estrogen exposure. *Mol. Endocrinol.* **27**, 1666-1677.

Johnson, M. H., Pickering, S. J., Braude, P. R., Vincent, C., Cant, A. and Currie, J. (1990). Acid Tyrode's solution can stimulate parthenogenetic activation of human and mouse oocytes. *Fertil. Steril.* **53**, 266-270.

Jones, K. T., Carroll, J. and Whittingham, D. G. (1995). Ionomycin, thapsigargin, ryanodine, and sperm induced Ca2+ release increase during meiotic maturation of mouse oocytes. *J. Biol. Chem.* **270**, 6671-6677.

Kang, D., Park, J.-Y., Han, J., Bae, I.-H., Yoon, S.-Y., Kang, S. S., Choi, W. S. and Hong, S.-G. (2003). Acetylcholine induces Ca2+ oscillations via m3/m4 muscarinic receptors in the mouse oocyte. *Pflugers Arch.* **447**, 321-327.

Kashir, J., Deguchi, R., Jones, C., Coward, K. and Stricker, S. A. (2013). Comparative biology of sperm factors and fertilization-induced calcium signals across the animal kingdom. *Mol. Reprod. Dev.* **80**, 787-815.

Kashir, J., Nomikos, M., Lai, F. A. and Swann, K. (2014). Sperm-induced Ca2+ release during egg activation in mammals. *Biochem. Biophys. Res. Commun.* **450**, 1204-1211.

Knott, J. G., Kurokawa, M., Fissore, R. A., Schultz, R. M. and Williams, C. J. (2005). Transgenic RNA interference reveals role for mouse sperm phospholipase Czeta in triggering Ca2+ oscillations during fertilization. *Biol. Reprod.* **72**, 992-996.

Liu, C., Li, Q., Zhou, X., Kolosov, V. P. and Perelman, J. M. (2013). Regulator of G-protein signaling 2 inhibits acid-induced mucin5AC hypersecretion in human airway epithelial cells. *Respir. Physiol. Neurobiol.* **185**, 265-271.

Ludwig, M.-G., Vanek, M., Guerini, D., Gasser, J. A., Jones, C. E., Junker, U., Hofstetter, H., Wolf, R. M. and Seuwen, K. (2003). Proton-sensing G-protein-coupled receptors. *Nature* **425**, 93-98.

Mayerhofer, A., Kunz, L., Krieger, A., Proskocil, B., Spindel, E., Amsterdam, A., Dissen, G. A., Ojeda, S. R. and Wessler, I. (2006). FSH regulates acetycholine production by ovarian granulosa cells. *Reprod. Biol. Endocrinol.* **4**, 37.

McGuinness, O. M., Moreton, R. B., Johnson, M. H. and Berridge, M. J. (1996). A direct measurement of increased divalent cation influx in fertilised mouse oocytes. *Development* **122**, 2199-2206.

Mehlmann, L. M. and Kline, D. (1994). Regulation of intracellular calcium in the mouse egg: calcium release in response to sperm or inositol trisphosphate is enhanced after meiotic maturation. *Biol. Reprod.* **51**, 1088-1098.

Mehlmann, L. M., Terasaki, M., Jaffe, L. A. and Kline, D. (1995). Reorganization of the endoplasmic reticulum during meiotic maturation of the mouse oocyte. *Dev. Biol.* **170**, 607-615.

Mehlmann, L. M., Mikoshiba, K. and Kline, D. (1996). Redistribution and increase in cortical inositol 1,4,5-trisphosphate receptors after meiotic maturation of the mouse oocyte. *Dev. Biol.* **180**, 489-498.

Mehlmann, L. M., Jones, T. L. Z. and Jaffe, L. A. (2002). Meiotic arrest in the mouse follicle maintained by a Gs protein in the oocyte. *Science* **297**, 1343-1345.

Mehlmann, L. M., Saeki, Y., Tanaka, S., Brennan, T. J., Evsikov, A. V., Pendola, F. L., Knowles, B. B., Eppig, J. J. and Jaffe, L. A. (2004). The Gs-linked receptor GPR3 maintains meiotic arrest in mammalian oocytes. *Science* **306**, 1947-1950.

Miao, Y.-L., Stein, P., Jefferson, W. N., Padilla-Banks, E. and Williams, C. J. (2012). Calcium influx-mediated signaling is required for complete mouse egg activation. *Proc. Natl. Acad. Sci. USA* **109**, 4169-4174.

Moore, G. D., Kopf, G. S. and Schultz, R. M. (1993). Complete mouse egg activation in the absence of sperm by stimulation of an exogenous G protein-coupled receptor. *Dev. Biol.* **159**, 669-678.

Pfaffl, M. W. (2001). A new mathematical model for relative quantification in real-time RT-PCR. *Nucleic Acids Res.* **29**, e45.

Roy, A. A., Lemberg, K. E. and Chidiac, P. (2003). Recruitment of RGS2 and RGS4 to the plasma membrane by G proteins and receptors reflects functional interactions. *Mol. Pharmacol.* **64**, 587-593.

Development (2015) 142, 2633-2640 doi:10.1242/dev.121707

Roy, A. A., Baragli, A., Bernstein, L. S., Hepler, J. R., Hébert, T. E. and Chidiac, P. (2006). RGS2 interacts with Gs and adenylyl cyclase in living cells. *Cell. Signal.* **18**, 336-348.

Runft, L. L., Jaffe, L. A. and Mehlmann, L. M. (2002). Egg activation at fertilization: where it all begins. *Dev. Biol.* **245**, 237-254.

Saunders, C. M., Larman, M. G., Parrington, J., Cox, L. J., Royse, J., Blayney, L. M., Swann, K. and Lai, F. A. (2002). PLC zeta: a sperm-specific trigger of Ca(2+) oscillations in eggs and embryo development. *Development* **129**, 3533-3544.

Saxena, H., Deshpande, D. A., Tiegs, B. C., Yan, H., Battafarano, R. J., Burrows, W. M., Damera, G., Panettieri, R. A., Dubose, T. D., Jr, An, S. S. et al. (2012). The GPCR OGR1 (GPR68) mediates diverse signalling and contraction of airway smooth muscle in response to small reductions in extracellular pH. *Br. J. Pharmacol.* **166**, 981-990.

Sinnarajah, S., Dessauer, C. W., Srikumar, D., Chen, J., Yuen, J., Yilma, S., Dennis, J. C., Morrison, E. E., Vodyanoy, V. and Kehrl, J. H. (2001). RGS2 regulates signal transduction in olfactory neurons by attenuating activation of adenylyl cyclase III. *Nature* **409**, 1051-1055.

Smiljaković, T., Josipović, S., Kosovac, O., Delić, N., Aleksić, S. and Petrović, M. M. (2008). The role of pH values in porcine reproductive tracts of male and female individuals. *Biotechnol. Anim. Husbandry* **24**, 101-108.

Stone, S. L. and Hamner, C. D. (1975). Biochemistry and physiology of oviductal secretions. *Gynecol. Obstet. Invest.* **6**, 234-252.

Tombes, R. M., Simerly, C., Borisy, G. G. and Schatten, G. (1992). Meiosis, egg activation, and nuclear envelope breakdown are differentially reliant on Ca2+, whereas germinal vesicle breakdown is Ca2+ independent in the mouse oocyte. *J. Cell Biol.* **117**, 799-811.

Wang, X., Huang, G., Luo, X., Penninger, J. M. and Muallem, S. (2004). Role of regulator of G protein signaling 2 (RGS2) in Ca(2+) oscillations and adaptation of Ca(2+) signaling to reduce excitability of RGS2−/− cells. *J. Biol. Chem.* **279**, 41642-41649.

Willars, G. B. (2006). Mammalian RGS proteins: multifunctional regulators of cellular signalling. *Semin. Cell Dev. Biol.* **17**, 363-376.

Williams, C. J., Schultz, R. M. and Kopf, G. S. (1992). Role of G proteins in mouse egg activation: stimulatory effects of acetylcholine on the ZP2 to ZP2f conversion and pronuclear formation in eggs expressing a functional m1 muscarinic receptor. *Dev. Biol.* **151**, 288-296.

Williams, C. J., Mehlmann, L. M., Jaffe, L. A., Kopf, G. S. and Schultz, R. M. (1998). Evidence that Gq family G proteins do not function in mouse egg activation at fertilization. *Dev. Biol.* **198**, 116-127.

Yalcin, B., Willis-Owen, S. A. G., Fullerton, J., Meesaq, A., Deacon, R. M., Rawlins, J. N. P., Copley, R. R., Morris, A. P., Flint, J. and Mott, R. (2004). Genetic dissection of a behavioral quantitative trait locus shows that Rgs2 modulates anxiety in mice. *Nat. Genet.* **36**, 1197-1202.

Zachariae, F. and Jensen, C. E. (1958). Studies on the mechanism of ovulation: histochemical and physico-chemical investigations on genuine follicular fluids. *Acta Endocrinol.* **27**, 343-355.

Supplementary Materials and Methods

Mice and breeding

The following mouse strains were used: CF-1 females (6-10 weeks, Harlan Laboratories), C57BL/6J females (6-10 weeks, Jackson Laboratories), and B6SJLF1/J males (2-6 months, Jackson Laboratories). Methods for the generation and genotyping of *Rgs2*$^{-/-}$ mice were reported previously (Oliveira-Dos-Santos et al., 2000). *Rgs2*$^{-/-}$ females, 6-10 weeks of age, were generously provided by Dr. Yaping Tu (Creighton Univ. School of Medicine). C57BL/6J females were used to obtain *Rgs2*$^{+/+}$ control eggs for ACh and ZP2 conversion experiments. For analysis of litter sizes, *Rgs2*$^{+/+}$ and *Rgs2*$^{-/-}$ mice were housed in breeding cages of one male with 1-3 females. Pregnant females were separated into individual cages prior to delivery, and pups were counted at birth. Litter data was collected for a period of 32 months from 8 (*Rgs2*$^{-/-}$ male x *Rgs2*$^{-/-}$ female) and 11 (*Rgs2*$^{+/+}$ male x *Rgs2*$^{+/+}$ female) breeding cages and for 10 months from 2 (*Rgs2*$^{-/-}$ male x *Rgs2*$^{+/+}$ female) breeding cages. All mice were maintained under approved protocols at each institution and complied with the Institute of Laboratory Animal Research Guide for the Care and Use of Laboratory Animals.

Culture media

In vitro maturation and post-injection culture were performed in minimal essential medium alpha (MEMα; Life Technologies) containing 5% calf serum (Atlanta Biologicals). For in vitro fertilization experiments, ZP-free eggs were loaded with 10 μM fura-2 AM (Life Technologies) in potassium simplex optimized medium (KSOM; EMD Millipore) containing 0.04% pluronic F-127 (Life Technologies) for 30 minutes. Eggs were adhered to Cell-Tak-coated (EMD Millipore) glass-bottom dishes in 90 μL BSA-free KSOM covered with mineral oil. Sperm were prepared in human tubal fluid (HTF; EMD Millipore) and were added to the imaging dish at a final concentration of 10^5 sperm/mL along with 4 μL HTF containing 30

mg/mL BSA to bring the final BSA concentration to 1.25 mg/mL. Acid and ACh addition experiments were performed in Leibovitz L-15 medium (L-15; Life Technologies). Ca^{2+}- and Mg^{2+}-free CZB medium without BSA or polyvinyl alcohol was prepared in-house (Chatot et al., 1989).

Ca^{2+} store measurements

Eggs were loaded with 10 μM fura-2 AM for 30 min in MEMα containing 5% calf serum and 0.04% pluronic F-127. The eggs were then washed and adhered to glass-bottom dishes in 2 mL of Ca^{2+}- and Mg^{2+}-free CZB without BSA or polyvinyl alcohol. In all experiments, control and experimental eggs were assayed at the same time in the same treatment dish. Baseline ratiometric imaging was performed for at least 5 min, followed by addition of thapsigargin to a final concentration of 10 μM. Imaging of F340 and F380 was performed as described previously (Miao et al., 2012). Area under the curve was measured for the first 10 min and was calculated using trapezoidal area for baseline-subtracted curves. Maximum amplitude was also determined relative to baseline measurements prior to thapsigargin addition. Both measurements were expressed relative to the mean value of control eggs from the same experiment.

Antibodies and DNA construct

Mouse monoclonal anti-RGS2 antibody (M01, clone 4C4; Abnova) was diluted 1:100. Rat monoclonal anti-ZP2 antibody (M2c.2) was kindly provided by Jurrien Dean (Rankin et al., 2003) and was diluted 1:500. Secondary antibody was peroxidase-conjugated anti-mouse or anti-rat IgG (Santa Cruz). FITC-conjugated anti-alpha-tubulin antibody (Sigma) was diluted 1:100 and rhodamine-phalloidin (Life Technologies) was used at a final concentration of 2 U/ml. The *HA-Rgs2* cRNA expression construct, in pcDNA3.1+, was obtained from Missouri S&T cDNA Resource Center (Rolla, MO).

Primers used

Rgs2 forward	5'-TTCTGGTTGGCTTGTGAAGA-3'
Rgs2 reverse	5'-CTTCTGAGCTGTGGTGAAGC-3'
Gpr68 forward	5'-CTCCTCCTCACCAGCTTCAA-3'
Gpr68 reverse	5'-CAGGTAAGGACAGCTAGGCA-3'
EGFP forward	5'-AGAACGGCATCAAGGTGAAC-3'
EGFP reverse	5'-TGCTCAGGTAGTGGTTGTCG-3'

Supplemental References

Chatot, C. L., Ziomek, C. A., Bavister, B. D., Lewis, J. L. and Torres, I. (1989). An improved culture medium supports development of random-bred 1-cell mouse embryos in vitro. *J. Reprod. Fertil.* **86**, 679-688.

Miao, Y. L., Stein, P., Jefferson, W. N., Padilla-Banks, E. and Williams, C. J. (2012). Calcium influx-mediated signaling is required for complete mouse egg activation. *Proc. Natl. Acad. Sci. USA* **109**, 4169-4174.

Oliveira-Dos-Santos, A. J., Matsumoto, G., Snow, B. E., Bai, D., Houston, F. P., Whishaw, I. Q., Mariathasan, S., Sasaki, T., Wakeham, A., Ohashi, P. S., et al. (2000). Regulation of T cell activation, anxiety, and male aggression by RGS2. *Proc. Natl. Acad. Sci. USA* **97**, 12272-12277.

Rankin, T. L., Coleman, J. S., Epifano, O., Hoodbhoy, T., Turner, S. G., Castle, P. E., Lee, E., Gore-Langton, R. and Dean, J. (2003). Fertility and taxon-specific sperm binding persist after replacement of mouse sperm receptors with human homologs. *Dev. Cell* **5**, 33-43.

SUPPLEMENTARY FIGURES

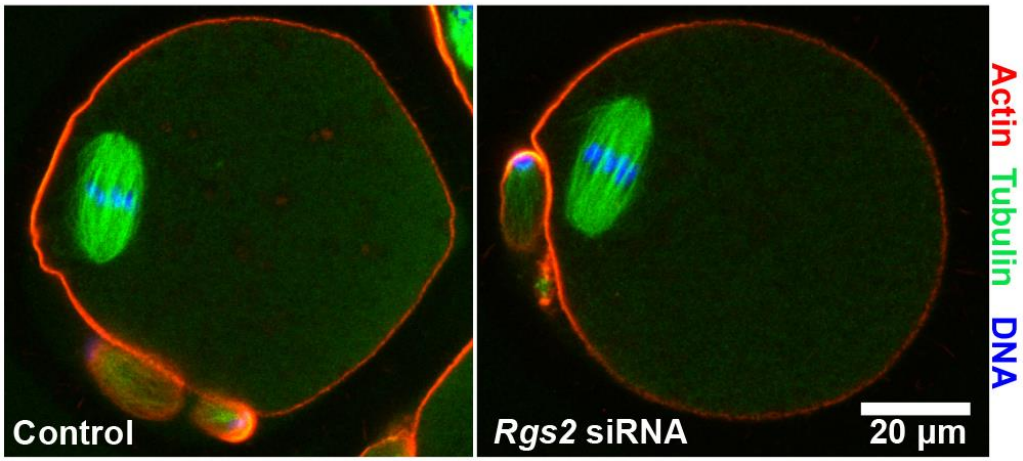

Figure S1. Normal oocyte maturation in eggs lacking RGS2. Oocytes were microinjected at the GV stage with scrambled siRNA (control) or *Rgs2* siRNA, then matured in vitro. A. Success of maturation of control and *Rgs2* siRNA-injected oocytes. Number of oocytes to reach the indicated stage out of the total maturing is shown. GVBD, germinal vesicle breakdown; MII, metaphase II. B. MII eggs were immunostained for actin (red), tubulin (green), and DNA (blue). Shown are representative images of 14-15 eggs per group. Scale bar: 20 µm.

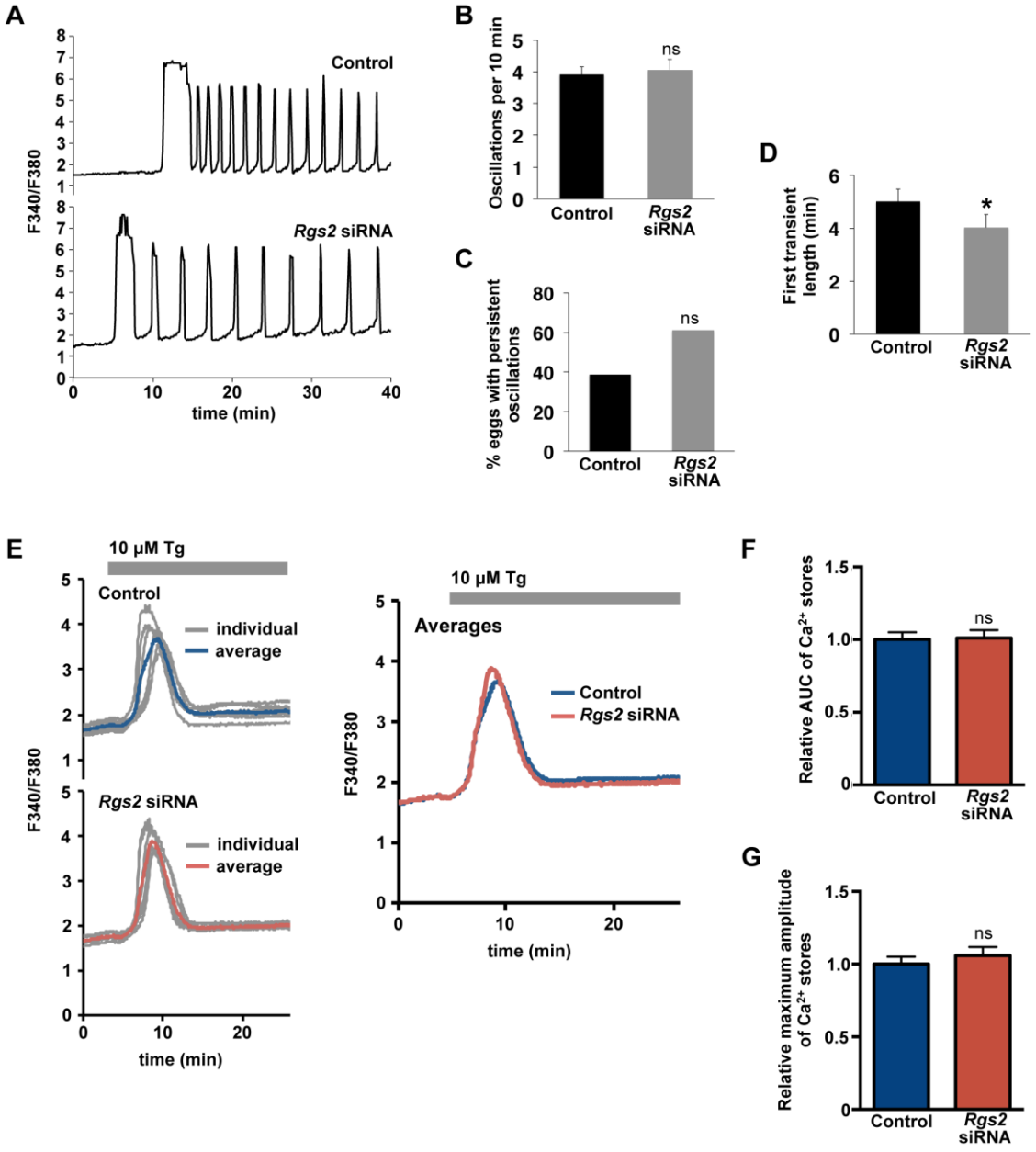

Figure S2. Ca^{2+} oscillatory patterns following fertilization and Ca^{2+} stores in eggs lacking RGS2. A. Representative Ca^{2+} tracings from eggs matured *in vitro* from control GV oocytes or oocytes microinjected with *Rgs2* siRNA. B. Oscillation frequency. Graph shows mean±s.e.m. of 31-36 eggs from 5 independent experiments. ns, no significant difference, Mann–Whitney *U*-test. C. Percentage of eggs with Ca^{2+} oscillations persisting for at least 60 min. Each column represents total of 31-36 eggs. ns, no significant difference, Chi square analysis. D. Duration of first Ca^{2+}

transient. Graph shows mean±s.e.m. of 34-41 eggs from 5 independent experiments. **P*<0.05, Mann–Whitney *U*-test. E. Representative traces of thapsigargin (Tg)-induced Ca^{2+} release for individual ZP-intact MII eggs (gray lines) and averages for 6 eggs (colored lines) are shown, along with the average traces shown together on one graph. F-G. Relative Ca^{2+} stores in ZP-intact control and *Rgs2* siRNA eggs. Graphs show mean±s.e.m. of area under the curve (AUC) (F) and maximum amplitude relative to baseline (G) for *N*=24-25 eggs from 4 independent experiments.

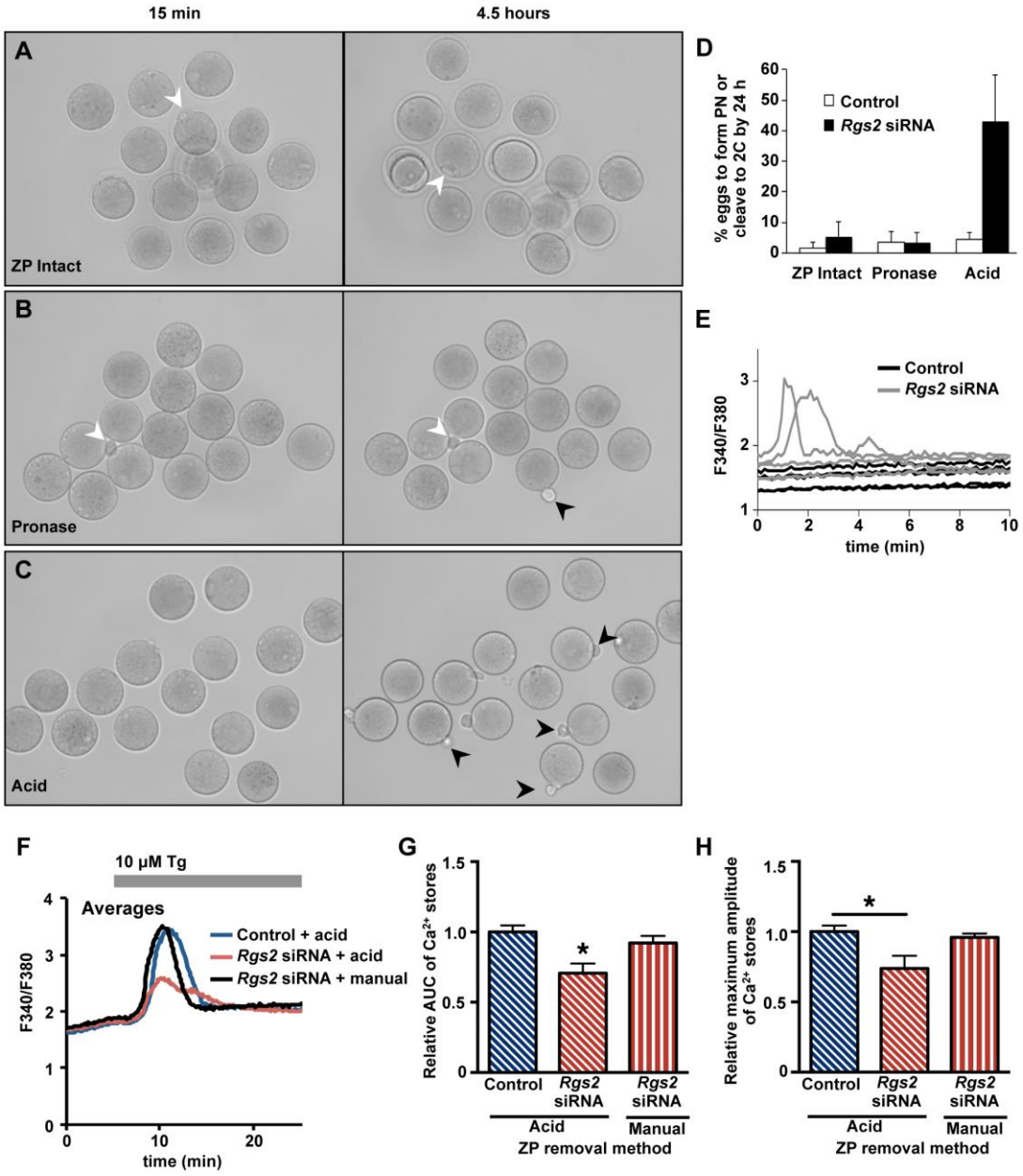

Figure S3. Effect of different methods of ZP removal on cell cycle resumption, Ca^{2+} release, and ER Ca^{2+} stores in eggs lacking RGS2. A-C. Photomicrographs of RGS2-depleted eggs at the indicated times following ZP removal. White arrowheads, first polar body; Black arrowheads, second polar body A. ZP not removed. B. ZP removed by pronase treatment. C. ZP removed using acid treatment. D. Percentage of pronuclear (PN) stage or 2-cell (2C) stage embryos following the indicated ZP removal method. Graph shows mean±s.e.m. of 8-19 eggs from 2-3

independent experiments. E. Ca^{2+} traces from control eggs or eggs lacking RGS2 (*Rgs2* siRNA) >1 hour following ZP removal using acid. Five representative traces are shown for each group. F. Thapsigargin (Tg)-induced Ca^{2+} release in ZP-free control and RGS2-depleted eggs following ZP removal using the indicated technique. Compiled average tracings of *N*=3-5 eggs/group are shown. G-H. Relative Ca^{2+} stores in control and *Rgs2* siRNA eggs. Graphs show mean±s.e.m. of 8-12 eggs/group from 2 independent experiments of area under the curve (AUC) (G) and maximum amplitude relative to baseline (H). **P*<0.05, one-way ANOVA with Tukey's multiple comparison test.

Table S1. Percentages of RGS2-depleted oocytes that underwent GVBD and developed to the MII stage.

	Control	*Rgs2* siRNA-injected
GVBD	64/64 (100%)	71/71 (100%)
MII	52/64 (81%)	56/71 (79%)